https://doi.org/10.5194/egusphere-2025-5564
Preprint. Discussion started: 10 February 2026

Inclusion of MyAMI-derived Mg/Ca corrections to the marine carbonate system in the cGENIE.cookie Earth system model (v.0.9.90)

Markus Adloff[1,2], Terra M. Ganey[3], Mathis P. Hain[3], Michael J. Henehan[2], Sarah E. Greene[1], Andy Ridgwell[4]

1 School of Geography, Earth and Environmental Sciences, University of Birmingham, Edgbaston, Birmingham, B15 2TT, United Kingdom
2 School of Earth Sciences, University of Bristol, Wills Memorial Building, Queens Road, Bristol, BS8 1RJ, United Kingdom
3 Earth and Planetary Sciences, University of California Santa Cruz, 1156 High Street, Santa Cruz, CA 95064, USA
4 Earth and Planetary Sciences, University of California Riverside, Geology 1242, 900 University Ave. Riverside, CA 92521, USA
Correspondence to: Markus Adloff (markus.adloff@bristol.ac.uk)

Abstract. The concentrations of the major cations (esp., Ca^{2+}, Mg^{2+}) in Earth's oceans have undergone large-scale fluctuations in the geological past. This is important because the key geochemical properties of the marine environment that underpin the global carbon cycle – the aqueous carbonate system equilibria and solubility of solid calcium carbonate ($CaCO_3$) – are heavily influenced by ion-pairing, which in turn depends on the activity of the major cations and anions. An accurate interpretation of marine proxies as well as the reconstruction of past states of ocean geochemistry and carbon cycle dynamics across geologic events requires that these effects are considered. However, most current global carbon cycle models use empirical carbonate system dissociation constants (K) fitted to laboratory experiments with present-day seawater major cation and anion concentrations. When simulations of global carbon cycling in the geologic past have been made, only relatively simplified empirical adjustments of the equilibrium constants (from Ben-Yaakov and Goldhaber [1974], Tyrrell and Zeebe [2004]) have been implemented when seawater composition differs from modern (e.g., *Panchuk et al.* [2008]). More commonly, no correction is made at all.

Here we develop and evaluate a new scheme in the cGENIE Earth system model for correcting carbonate system equilibrium constants and account for variations in the dissolved calcium and magnesium concentrations in the ocean. We base our new parameterization on the MyAMI specific ion interaction model of Hain et al. [2015] and implement this in cGENIE by means of linear interpolation within a 4-dimensional parameter look-up table of pre-calculated carbonate system equilibrium constants. For modern SW composition, our implementation of MyAMI-based equilibrium constants yields no significant deviation from model results using empirically-based equilibrium constants, validating our look-up/interpolation approach. However, for simulations conducted under non-modern Mg/Ca, we find significant differences in carbon chemistry and $CaCO_3$ saturation when using our new MyAMI-based equilibrium constants as compared to the existing (default) correction scheme. Specifically, our new MyAMI-based correction scheme exhibits a much lower sensitivity of surface ocean *p*H and calcite saturation state to a change in Mg/Ca from modern to Eocene, which were overestimated by the previous correction scheme. We can also expect that any bias in carbonate chemistry and $CaCO_3$ saturation will affect the preservation and burial of $CaCO_3$ in deep-sea sediments. We illustrate this by contrasting the ocean carbon inventory arising under Eocene Mg/Ca with the same total weathering

https://doi.org/10.5194/egusphere-2025-5564
Preprint. Discussion started: 10 February 2026

(and hence $CaCO_3$ burial) flux for the different possible equilibrium constant corrections. We find that the new MyAMI-based and previous default corrections give rise to a dissolved inorganic ocean carbon inventory 348 PgC higher and 950 PgC lower, respectively, relative to the same experiment conducted using empirical equilibrium constants without any Mg/Ca correction. Applying no correction at all for a different-from-modern Mg/Ca ratio in the ocean would appear to be better than applying a 'bad' correction but explicitly accounting for past dissolved calcium concentrations remains of fundamental importance. We provide this new carbonate system equilibria correction as an option in cGENIE.muffin version 0.9.64, and as standard in a completely new cGENIE code release – cGENIE.cookie v.0.9.

https://doi.org/10.5194/egusphere-2025-5564
Preprint. Discussion started: 10 February 2026

1. Introduction

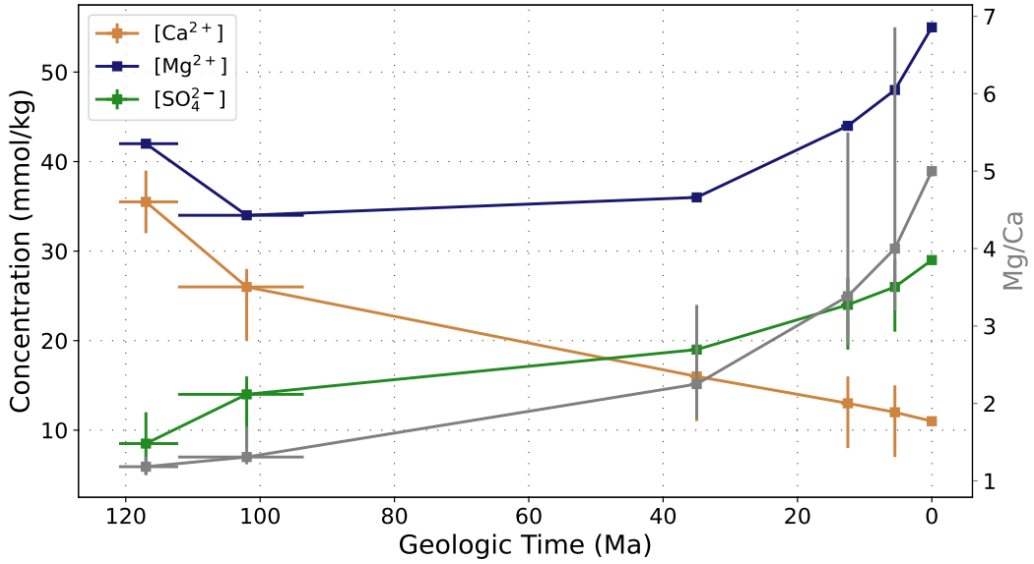

Figure 1: Changes of seawater [Mg2+], [Ca2+], [SO42-] and Mg/Ca since the Cretaceous as reconstructed from halite inclusions (Timofeeff et al. [2006], Brennan et al. [2013]).

The major ion (Na^+, K^+, Ca^{2+}, Mg^{2+}, Cl^-, SO_4^{2-}) composition of the ocean has changed substantially through Earth history (e.g., Horita et al. [1991], Hardie et al. [1996], Fig. 1). For example, the Ca^{2+} concentration ($[Ca^{2+}]$) was higher during the Cretaceous (up to ~33 mmol kg^{-1} compared to 10 mmol kg^{-1} today) while $[Mg^{2+}]$ was lower (35-40 mmol kg^{-1} compared to 52 mmol kg^{-1} today, Timofeeff et al. [2006], Brennan et al. [2013], Hain et al. [2015]). The first order consequence of higher Cretaceous $[Ca^{2+}]$ (as we will illustrate later) is that to produce a relatively similar ocean surface carbonate saturation state (or global weathering rate) to the present day, the ocean carbonate ion (CO_3^{2-}) concentration would have been lower as carbonate saturation involves the product of both $[Ca^{2+}]$ and $[CO_3^{2-}]$ (Ridgwell [2005], Ridgwell and Zeebe [2005]). In turn, lower $[CO_3^{2}]$ creates a seawater carbonate system that would have been less buffered against a rise in CO_2 (Hain et al. [2015]). The existence of higher Cretaceous $[Ca^{2+}]$ also allows elevated (compared to modern) atmospheric pCO_2 and reduced ocean surface pH (e.g., Henehan et al. [2019]) to be reconciled with an abundance of geological carbonate deposits and absence of an 'ocean acidification' crisis amongst marine calcifying organisms (Hönisch et al. [2012]). Changing proportions of $[Mg^{2+}]$ vs. $[Ca^{2+}]$ (hereafter: Mg/Ca) have been linked to major changes in the dominant mineralogy of carbonate-precipitating organisms (Hardie [1996]; Stanley and Hardie [1998]; Stanley et al. [2005]; Stanley [2006]), with calcite precipitation favoured in low-$[Mg^{2+}]$ seawater (such as during the Cretaceous) but calcite precipitation inhibited in favour of the aragonite polymorph in higher Mg/Ca modern seawater (e.g., Berner [1975], Morse et al. [2007]).

$[Ca^{2+}]$ and $[Mg^{2+}]$ have additional but much less appreciated impacts on the aqueous equilibria of carbon: both contribute to the ionic strength of seawater, they both significantly interact with carbonate species and borate (Millero and Thurmond [1983]; Harvie et al. [1984]), and they both can form complexes with carbonate, bicarbonate and hydroxide ion (Larsen et al. [1973]; Harvie et al. [1984]; Pitzer [1991]; Stefánsson et al. [2017]). As a result, $[Ca^{2+}]$ and $[Mg^{2+}]$ significantly affect the activity coefficients of free anions, the proportion of free and complexed anions, as well as the

https://doi.org/10.5194/egusphere-2025-5564
Preprint. Discussion started: 10 February 2026

value of the equilibrium constants determining carbon speciation, CO_2 fugacity and $CaCO_3$ saturation state of seawater. While environmental (temperature, salinity, pressure) controls on the carbonate system equilibrium are accounted for in empirically-determined modern seawater equilibrium constants, equilibrium constants for paleo-seawater also need to be adjusted to account for different $[Ca^{2+}]$ and $[Mg^{2+}]$ (Hain et al. [2015]). This is relevant in reconstructions of atmospheric CO_2 from B isotope-based seawater *p*H, when solving the carbonate system in Earth System models, and especially when using reconstructed *p*H to validate simulated past global carbon cycle states and carbon-climate dynamics occurring on geological timescales. The necessary corrections can be computed using Pitzer-type models based on potentiometric data (Pitzer [1991]; Millero and Pierrot [1998]; Hain et al. [2015]; Clegg et al. [2023]).

The 'muffin' release of the Earth system model of intermediate complexity 'cGENIE' (Ridgwell et al. [2007]) has been widely used to generate realizations of marine carbon cycling and atmospheric pCO_2 for a variety of geological intervals and events as well as for carrying out model-data comparison against carbon cycle-related paleoceanographic proxies (e.g., Gutjahr et al. [2017]; Greene et al. [2019]). The-atmosphere-ocean-sediment biogeochemistry originally developed in cGENIE was calibrated against spatial observations of modern ocean geochemistry (Ridgwell et al. [2007]) and surface sediment composition (Ridgwell and Hargreaves [2007]) and based on carbonate chemistry understanding rooted in modern seawater composition (Ridgwell [2001]). The first paleo application of cGENIE was a study constraining the carbon release to the ocean and atmosphere associated with the Paleocene-Eocene Thermal Maximum warming event (ca. 55 Ma) and involved directly contrasting simulated model with observed deep-sea sedimentary calcium carbonate ($CaCO_3$) contents across the event (Panchuk et al. [2008]). In this study, the potential importance of higher ocean $[Ca^{2+}]$ (18.2 mmol kg^{-1}) and lower $[Mg^{2+}]$ (29.9 mmol kg^{-1}) during the early Eocene in modifying carbonate preservation and burial in marine sediments, was recognized. Following Tyrrell and Zeebe [2004], two adjustments were made to the aqueous carbonate chemistry scheme of *Ridgwell et al.* [2007] (described in the S.I. of Panchuk et al. [2008]), which at the time represented the state-of-the-art in (paleo) carbon cycle modelling.

1. Firstly, the solubility coefficient for calcite was adjusted as a function of the deviation of ambient Mg/Ca from a modern reference Mg/Ca value (Tyrrell and Zeebe [2004]).

(E1) $$K_{sp} = K_{sp,modern} - \alpha \cdot \left(\frac{[Mg^{2+}]_{modern} - [Mg^{2+}]}{[Ca^{2+}]_{modern} - [Ca^{2+}]} \right)$$

where K_{sp} is the solubility coefficient of calcite for a modern seawater composition (Mucci, 1983), $[Mg^{2+}]_{modern}$ and $[Ca^{2+}]_{modern}$ are the modern mean seawater concentrations (52.82 and 10.25 mmol kg^{-1}, respectively), and $\alpha = 3.655 \times 10^{-8}$ is a scaling constant.

2. Secondly, because of the tendency of Mg^{2+} to form ion pairs in seawater (Zeebe and Wolf-Gladrow [2001]), the 1st and 2nd equilibrium constants of carbonic acid (K_1, K_2) were scaled as a function of the relative deviation of $[Mg^{2+}]$ from modern, following Ben-Yaakov and Goldhaber [1973].

(E2) $$K_{(x)} = \left(1 + s_{K(x)} \cdot \frac{[Mg^{2+}] - [Mg^{2+}]_{modern}}{[Mg^{2+}]_{modern}}\right) \cdot K_{(x),modern}$$

where $K_{(x),modern}$ is the equilibrium constant for modern seawater composition (in cGENIE – Mehrbach et al. [1973] as refit by Dickson and Millero [1987]), and $s_{K(x)}$ is a sensitivity parameter. *x* is either 1 or 2 –

https://doi.org/10.5194/egusphere-2025-5564
Preprint. Discussion started: 10 February 2026

corresponding to K_1 or K_2. The values of $s_{K(x)}$ are 0.155 and 0.442 for K_1 and K_2, respectively (Ben-Yaakov and Goldhaber [1973]).

This correction has been employed in subsequent cGENIE.muffin paleo studies (e.g., Gutjahr et al. [2017]; Greene et al. [2019]). However, the availability of recently developed seawater chemical speciation models now leads us to re-visit the existing scheme in cGENIE, and implement and fully evaluate an updated correction scheme for use in paleo studies.

The current state-of-the-art in seawater chemical speciation modelling combines the classical ion-pairing approach (Sillen [1961]; Garrels and Thomas [1962]; Morel and Morgan [1972]; Millero and Schreiber [1982]) with specific ion interaction modelling of the free ions (Pitzer [1991]). This approach was implemented as the 'MIAMI' spreadsheet model and which compared well when evaluated against empirical measurements of standard modern seawater by Millero and Pierrot [1998]. MIAMI builds on a substantial empirical database of dissociation constants in artificial and, particularly for K_1 and K_2, natural seawater (Millero and Pierrot [1998]; Millero et al., [2002]). It is a comprehensive and often-used model to calculate chemical speciation specifically in seawater (Turner et al. [2016]). A simplified version of MIAMI was re-implemented (MyAMI) in the Python language by Hain et al. [2015] to make the approach more accessible to paleo seawater studies and Earth System modelling. To reduce the computational effort required in MIAMI, MyAMI only contains Pitzer equations for the activities of the species most relevant for the carbonate system. Furthermore, these were shortened by removing the higher-order electrostatic terms that are more relevant for media with much more elevated ionic strength than open ocean seawater. MyAMI enables carbonate system equilibria to be solved for a wide range of temperatures, salinities, $[Mg^{2+}]$ and $[Ca^{2+}]$ (assuming the modern seawater relationship between salinity and ionic strength). MyAMI predicts the dissociation constants of the carbonate system in the present-day ocean with an error of just a few percent (Hain et al. [2015]) and was, at the time calibrated against the best-practice modern seawater empirical equilibrium constants (chapter 5, section 7 in Dickson et al. [2007]). (Subsequently, Zeebe and Tyrrell [2018] recognized an inaccuracy in the K_1 predicted by MyAMI, and this issue was resolved by replacing the literature source for the calcium-bicarbonate interaction parameters (Hain et al. [2018]; https://github.com/MathisHain/MyAMI).) MyAMI-derived corrections to the temperature- and salinity-dependencies of the equilibration constants are available in Seacarbx (Raitzsch et al. [2022]), cbsyst (Brason et al. [2023]), and KGEN (Whiteford et al. [2025]) and are commonly used to reconstruct local carbonate system parameters for the late Cretaceous through the Cenozoic (e.g., Sosdian et al. [2018], Anagnostou et al. [2020], Rae et al. [2021]; CenCO2PIP [2023]). However, MyAMI-derived equilibrium constants have not yet been incorporated into 3D ocean-based Earth system models, particularly those used to infer states of global carbon cycling from local sediment observations. Instead, some, like cGENIE, rely on older correction schemes that only partially account for major ion effects (Hain et al. [2015]) or do not consider effects of major ion changes at all.

In this paper, we describe and evaluate an implementation of MyAMI-derived carbonate system constants including the effect of different-from-modern $[Ca^{2+}]$ and $[Mg^{2+}]$ in the cGENIE.cookie Earth system model.

https://doi.org/10.5194/egusphere-2025-5564
Preprint. Discussion started: 10 February 2026

2. Methods

We start by providing a full description of how the cGENIE Earth system model represents aqueous carbonate chemistry. We then describe how the major equilibrium constants are derived from MyAMI, and then implemented in cGENIE as an alternative option for solving the aqueous carbonate system. Finally, we describe our testing and evaluation methodology for the MyAMI-enabled marine carbon cycle in cGENIE and how this compares both to the current Mg/Ca correction scheme as well as to not accounting for different-from-modern ocean Mg/Ca ratios at all. Note that 'muffin' (original) and 'cookie' (new) releases of cGENIE differ only in the criteria for $[H^+]$ convergence (described below) and whether or not the MyAMI-based correction scheme is employed by default (*cookie*) or only as an option that needs to be specified (*muffin*).

2.1 The cGENIE Earth system model

Aqueous carbonate chemistry in cGENIE is governed by two tracers in the ocean circulation model – (1) dissolved inorganic carbon (DIC) which is the sum of: $CO_{2(aq)}$ (ignoring the contribution from carbonic acid $H_2\ CO_3$), HCO_3^- (bicarbonate ions), and CO_3^{2-} (carbonate ions), and (2) alkalinity (ALK) which is defined following *Dickson* [1981] (see Equation E13, below).

The default empirical fits employed in cGENIE for the 1st and 2nd dissociation constants of carbonic acid,

(E3) $$K_1 = \frac{[H^+]\cdot[HCO_3^-]}{[H_2O]\cdot[CO_2]}$$

(E4) $$K_2 = \frac{[H^+]\cdot[CO_3^{2-}]}{[HCO_3^-]}$$

are those of *Mehrbach et al.* [1973] as refitted by *Dickson and Millero* [1987] (*muffin*) and are a function of the ambient environmental conditions of temperature (T) and salinity (S). Note that all *K*s in this manuscript are the stoichiometric (or apparent) dissociation constants.

Strictly speaking, the empirically-determined equations for the various dissociation (and stability) constants are valid only over the range of experimental conditions from which they were derived. For K_1 and K_2 from *Mehrbach et al.* [1973] (refit by *Dickson and Millero,* [1987]) – the current default choice in *c*GENIE.muffin – T and S are limited to the range: $2 \le T \le 35$°C, and $26 \le S \le 43$ PSU. Model-projected values of T and/or S lying outside of this range are simply truncated at the minimum or maximum empirical limits for the purpose of the carbonate chemistry calculation. For consistency, the same T and S range limitations as for K_1 and K_2 are placed on all other dissociation (and carbonate stability) constants. Note that the default environmental limits associated with calculating Bunsen gas solubility coefficients are $2 \le T \le 35$ °C and $26 \le S \le 43$ PSU (and which are left unchanged throughout the experiments in this paper), while the temperature limits for calculating the Schmidt numbers used in air-sea gas transfer are $0 \le T \le 30$°C, following *Wanninkhof* [1992].

cGENIE solves for acidity on the seawater *p*H scale (pH_{SWS}), with all dissociated constants converted to pH_{SWS} if originally fitted on a different scale. Numerical solution of the carbonate system is via an implicit iterative method to obtain the equilibrium hydrogen ion concentration ($[H^+]$). Iteration n+1 of this calculation depends on the results of the previous iteration (n) via:

https://doi.org/10.5194/egusphere-2025-5564
Preprint. Discussion started: 10 February 2026

$$(E5)\ [H^+]_{n+1} = \left([H^+]_n^{K_1}{}^2 + [H^+]_n^{K_1}{}^2 \right)^{0.5}$$

where:

$$(E6)\ [H^+]_n^{K_1} = K_1 \cdot [CO_2]_n / [HCO_3^-]_n$$

$$(E7)\ [H^+]_n^{K_2} = K_2 \cdot [HCO_3^-]_n / [CO_3^{2-}]_n$$

In turn, the concentrations of: CO_2, HCO_3^-, and CO_3^{2-} in the n^{th} iteration are estimated from *Skirrow* [1975]:

$$(E8)\ CO_{2,n} = DIC_n - ALK_{DIC,n} + \frac{k\cdot(ALK_{DIC,n} - DIC_n) - 4.0\cdot ALK_{DIC,n} + z_n}{2.0\cdot(k-4.0)}$$

$$(E9)\ HCO_{3,n}^- = \frac{k\cdot DIC_n - z_n}{k-4.0}$$

$$(E10)\ CO_{3,n}^{2-} = \frac{k\cdot(ALK_{DIC,n} - DIC_n) - 4.0\cdot ALK_{DIC,n} + z_n}{2.0\cdot(k-4.0)}$$

where:

$$(E11)\ z_n = \left((4.0-k)\cdot ALK_{DIC,n} + k\cdot DIC_n \right)^2 + \left(4\cdot(k-4.0)\cdot (ALK_{DIC,n})^2 \right)^{0.5}$$

and

$$(E12)\ k = \frac{K_1}{K_2}$$

We define carbonate alkalinity, ALK_{DIC}, using the full alkalinity definition of *Dickson* [1990], but excluding only the contribution from S^{2-} (which is important only at very low values of *p*H; *Zeebe and Wolf-Gladrow* [2001]):

$$(E13)\ ALK_{DIC,n} = ALK - H_4BO_4^- - OH^- - HPO_4^{2-} - 2.0\cdot PO_4^{3-} - H_3SiO_4^- - NH_3 - HS^- + H^+ + HSO_4^- + HF + H_3PO_4$$

In calculating these components, we use the apparent ionization constant of boric acid (K_B) from *Dickson* [1990];

$$(E14)\ K_B = \frac{[H^+]\cdot[H_4BO_4^-]}{[H_2O]\cdot[H_3BO_3]}$$

converting from the original total *p*H scale to the seawater *p*H scale (*Millero* [1995], and the apparent ionization constant of water (K_B) from *Millero* [1992] (fitted on pH_{SWS} scale):

$$(E15)\ K_H = \frac{[H^+]\cdot[OH^-]}{[H_2O]}$$

The 1st, 2nd, and 3rd dissociation constants of phosphoric acid, as well as the dissociation constants of silicic acid and ammonium, are all from *Yao and Millero* [1995] (and were all originally fitted on the pH_{SWS} scale).

$$(E16)\ K_{P1} = \frac{[H^+]\cdot[H_2PO_4^-]}{[H_3PO_4]}$$

$$(E17)\ K_{P2} = \frac{[H^+]\cdot[HPO_4^{2-}]}{[H_2PO_4^-]}$$

https://doi.org/10.5194/egusphere-2025-5564
Preprint. Discussion started: 10 February 2026

(E18) $K_{\mathrm{P3}} = \frac{[\mathrm{H^+}]\cdot[\mathrm{PO_4^{3-}}]}{[\mathrm{HPO_4^{2-}}]}$

(E19) $K_{\mathrm{NH4}} = \frac{[\mathrm{H^+}]\cdot[\mathrm{NH_3}]}{[\mathrm{NH_4^+}]}$

(E20) $K_{\mathrm{Si}} = \frac{[\mathrm{H^+}]\cdot[\mathrm{H_3SiO_4^-}]}{[\mathrm{H_4SiO_4}]}$

The dissociation constant of hydrogen sulphide is from *Millero et al.* [1988] (converting from total to seawater *p*H scale);

(E21) $K_{\mathrm{H2S}} = \frac{[\mathrm{H^+}]\cdot[\mathrm{HS^-}]}{[\mathrm{H_2S}]}$

the dissociation constant of bisulfate is from *Dickson* [1990] (converting from free to seawater *p*H scale),

(E22) $K_{\mathrm{HSO4}} = \frac{[\mathrm{H^+}]\cdot[\mathrm{SO_4^{2-}}]}{[\mathrm{HSO_4^-}]}$

and for HF, we adopt the dissociation constant of hydrogen fluoride from *Dickson and Riley* [1979] and convert from the free to seawater *p*H scale:

(E23) $K_{\mathrm{HF}} = \frac{[\mathrm{H^+}]\cdot[\mathrm{F^-}]}{[\mathrm{HF}]}$

In solving the carbonate system, the initial $[H^+]$ value ($[H^+]_{n=1}$) everywhere in the ocean is seeded with an approximately representative bulk ocean value of $10^{-7.8}$ (*p*H = 7.8) at the start of a model experiment. Thereafter, the initial $[H^+]$ value each time (and time-step) in which the carbonate system is solved is taken from the equilibrium value calculated at the previous time-step at the same ocean model grid point. We judge the system to be sufficiently converged when $[H^+]$ changes by less than 0.01% between iterations which brings *p*H and fCO_2 to within ±0.001 units (pH_{SWS}) and ±0.2 µatm, respectively, compared to a fully converged solution (*muffin*). In cookie, we assume a *p*H convergence threshold of 0.001 units (pH_{SWS}). This scheme is generally stable for plausible (including future and deep geological time) differences between DIC and ALK. Extreme ratios of DIC:ALK or ALK < ca. 500 µmol eq. kg^{-1} (less than 25% of modern) can lead to numerical instability if the two independent $[H^+]$ estimates (E6, E7) are sufficiently far apart. By default, *p*H (including constants) is only recalculated every time-step in the ocean surface grid points in the model. At the seafloor, if the sediment model (e.g., *Ridgwell and Hargreaves* [1997]) is used, *p*H is updated on an annual average. Otherwise, *p*H is only solved in the ocean interior if required in providing model output, or if ocean interior carbonate speciation is required such as in the case of methanotrophy (*Reinhard et al.* [2020].

Dissolved Ca^{2+} and total SO_4^{2-} (HSO_4^- + SO_4^{2-}) are typically configured as prognostic tracers in cGENIE model experiments, in which case their oceanic distributions are simulated explicitly. If not selected, their concentrations are estimated from salinity following *Millero* [1982, 1995]):

(E24) $[Ca^{2+}] = 0.01028 \cdot \frac{S}{35.0}$

(E25) $\left[SO_{4(\mathrm{tot})}\right] = 0.000416 \cdot \frac{S}{35.0}$

Even if sulfate is carried as an explicit tracer in the model, for internally correcting stability constants between different *p*H scales, $[SO_4^{2-}]$ is always derived using the modern relationship with salinity as above (Equation E25). The justification for this is that the stability constants used in cGENIE, including the new MyAMI-derived ones, are all based on a modern

https://doi.org/10.5194/egusphere-2025-5564
Preprint. Discussion started: 10 February 2026

seawater sulfate composition so as to avoid bias when calculating pH on the total scale. Note that the explicit tracer concentration of sulfate, if available, is used in the calculation of ALK_{DIC} (Equation E13 above).

The concentrations of total boric acid and fluorine are typically not included as prognostic tracers in cGENIE model experiments, and are estimated from salinity following *Millero* [1982, 1995]:

$$(E26)\ \left[B_{(tot)}\right] = 0.000416 \cdot \frac{S}{35.0}$$

$$(E27)\ \left[F_{(tot)}\right] = 0.00007 \cdot \frac{S}{35.0}$$

If a marine cycle of silica and hence the tracer silicic acid (H_4SiO_4) is not included in a given experiment configuration, a zero concentration is assumed throughout the ocean. For the modern ocean, the error in atmospheric CO_2 induced by this simplification compared to a carbon cycle utilizing observed H_4SiO_4 concentrations is < 1 µatm (*Ridgwell* [2001]. Note that if the H_4SiO_4 tracer is included but used as a diagnostic tracer for tracking rates of silicate weathering and there is no corresponding opal sink (e.g., *Hülse and Ridgwell* [2025]), it can be omitted from the calculation of ALK_{DIC} so as to avoid unintended impacts on ocean *p*H.

Finally, the saturation index (or 'saturation state') with respect to $CaCO_3$, W, is defined as the product of calcium and carbonate ion concentrations divided by solubility product K_{sp}, where seawater with Ω > 1 is oversaturated and Ω < 1 undersaturated with respect to $CaCO_3$:

$$(E28)\ \Omega = \frac{[Ca^{2+}][CO_3^{2-}]}{K_{sp}}$$

The solubility products for calcite and aragonite, $K_{sp,cal}$ and $K_{sp,arg}$, respectively, are from *Mucci* [1983] and the corresponding saturation states are given the notation W_{cal} and W_{arg}, respectively.

All dissociation constants are corrected for pressure (*P*) following *Millero* [2005] and assuming that we can approximately relate depth below the ocean surface and pressure as 1 dbar m^{-1} (which induces an error of no more than ~3% even at the deepest depths of the modern ocean [*Ridgwell*, 2001]). Corrections are applied to all dissociation constants used in cGENIE – K_1, K_2, K_B, K_W, K_{Si}, K_{HF}, K_{HSO4}, K_{H2S}, K_{NH4}, K_{P1}, K_{P2}, and K_{P3}, plus $K_{sp,cal}$ and $K_{sp,arg}$. Following *Millero* [1979], the general form of the pressure correction factor is:

$$(E29)\ ln\left(\frac{K_{(P)}}{K_{(0)}}\right) = -\left(\frac{\Delta V}{R \cdot T}\right) \cdot P + \left(\frac{0.5 \cdot \Delta\kappa}{R \cdot T}\right) \cdot P^2$$

where *P* is the applied pressure in bars, *T* is the temperature (°C), D*V* and Dk are the molar volume and compressibility change for the dissociation reactions, respectively, and *R* is the gas constant (83.145 bar cm^3 mol^{-1} K^{-1}). For each dissociation reaction the values of D*V* and Dk in seawater are approximated as function only of temperature (assuming a salinity of 35 PSU) by

$$(E30)\ \Delta V = a_0 + a_1 \cdot T + a_2 \cdot T^2$$

$$(E31)\ 10^3 \cdot \Delta\kappa = b_0 + b_1 \cdot T$$

using the coefficients a_0 … b_1. In the absence of an available relationship describing the effect of pressure on the dissociation of silicic acid, the same pressure effect as for boric acid is assumed.

https://doi.org/10.5194/egusphere-2025-5564
Preprint. Discussion started: 10 February 2026

The values of the various coefficients are corrected for historical typographical errors in the literature where necessary (see *Lewis and Wallace* [1998] for an overview of some (but not all) of the typos prevalent in the literature, and *Orr et al.* [2015] for a more recent intercomparison of packages solving the aqueous carbonate system and corrected coefficient values). We detail all the dissociation constant coefficients used in *c*GENIE in Table SI.1. Pressure corrections to the various dissociation constants are formulated based on *Lewis and Wallace* [1998] (also see *Orr et al.* [2015]). Again, because of the occurrence of typographical errors in the literature, we also, for completeness, detail all the pressure correction coefficients used in *c*GENIE in Table SI.2.

2.2 Implementation of MyAMI-derived lookup tables in cGENIE

Since $[Mg^{2+}]$ and $[Ca^{2+}]$ are spatially and temporally variable in the ocean, a direct application of MyAMI in cGENIE would require running MyAMI for every grid cell and at every time step in order to solve the carbonate system for the current boundary conditions. This process would be excessively computational expensive, and hence we did not incorporate the MyAMI code (Python) itself into cGENIE (F77, f90). Also, to quantitatively evaluate the overall effects of using MyAMI rather than the previous default correction scheme requires backward-compatibility, precluding a complete revision of the carbonate chemistry solver codebase of cGENIE. Therefore, we followed the approach of *Ridgwell et al.* [2003] (in that particular case, sediment dissolution fluxes were pre-calculated as a function of 5 different boundary conditions and substituted for a mechanistic 1D reaction-transport model for the seafloor flux) and generated look-up tables of carbonate system equilibrium constants under various boundary conditions, with the gridded values created through offline calculations with MyAMI. The gridded values are included in the cGENIE source code repository in the form of an ASCII format file for each equilibrium constant that is read in by the cGENIE model at runtime. The equilibrium constants are quadri-linearly interpolated from the look-up table using run-time environmental conditions (T, S, $[Ca^{2+}]$, $[Mg^{2+}]$) in each ocean model grid-cell. We validate the accuracy of this implementation in section 3.1 below.

We generated one look-up table for each of the equilibrium constants: K_1, K_2, K_w, K_B, K_{HSO4} $K_{sp,arg}$, and $K_{sp,cal}$. To create these values, the MyAMI model version 1.0 (Hain et al. [2015, 2018]) was run for all combinations of seawater temperature (-2 – 50°C in 1°C steps), salinity (30 – 45 PSU in 1 PSU steps), $[Ca^{2+}]$ (1 – 60 mmol kg^{-1} in 1 mmol $^{-1}$ steps) and $[Mg^{2+}]$ (1 – 60 mmol/kg in 1 mmol/kg steps). For environmental conditions at any location in the cGENIE ocean grid falling outside of these limits, no extrapolation is applied, and parameter values are capped at the limit value. Compared to the default *Mehrbach et al.* [1973] equilibrium constants, the permissible range in T and S in this new parameterization is now expanded to $-2 \leq T \leq 50$°C, and $30 \leq S \leq 45$ PSU (instead of $2 \leq T \leq 35$°C, and $26 \leq S \leq 43$ PSU). When the MyAMI constants are selected in the cGENIE model, this range is applied to all equilibrium constants. The ranges for Bunsen gas solubility coefficients and Schmidt numbers are left at their defaults (see earlier).

To retain backwards compatibility, MyAMI carbonate dissociation constants are used in place of *Mehrbach et al.* [1973] if explicitly selected by the user in *muffin* but become the defaults in *cookie*. When MyAMI is enabled, the original (*muffin*) carbonate dissociation constants, including the $[Mg^{2+}]$ and $[Ca^{2+}]$ corrections of *Ben-Yaakov and Goldhaber* [1973] and *Tyrell and Zeebe* [2004], are simply replaced with ones derived from MyAMI. For compatibility with the *p*H units used in cGENIE, we convert the MyAMI-derived constants from the total to the seawater *p*H scale, and from molarities (mol per kg pure water solvent) to amount concentrations (mol per kg seawater). Further, we combine K_0 and

https://doi.org/10.5194/egusphere-2025-5564
Preprint. Discussion started: 10 February 2026

K_1 from the MyAMI output as is done in the default carbonate system scheme in cGENIE to treat H_2CO_3 implicitly (Pines et al. [2016]):

(E32) $$\log k_{GENIE} = \log k_{1,GENIE} + {}^{1}/_{\log k_{0,GENIE}}$$

The interpolated constants are then pressure-corrected consistent with other cGENIE carbonate constants with the pressure correction carried out via partial volumes and compressibility parameters taken from *Millero et al.* [1979, 1983 and 1995].

Note that we did not change [SO_4^{2-}] from modern in the current study. An expansion of the carbonate system solver to correct for varying [SO_4^{2-}] will be a focus of future model development.

2.3 Implementation of calcium carbonate diagenesis in cGENIE

The lookup table approach to calculating $CaCO_3$ dissolution in surface sediments of the deep ocean (and hence carbonate burial) (*Ridgwell and Hargreaves* [2007]), although able to account for changing ocean [Ca^{2+}], is uncorrected for deviations in Mg/Ca from modern (*Ridgwell* [2001]). For paleo seawater compositions, cGENIE.cookie explicitly employs the (f77 converted to f90) code of *Archer* [1991] in calculating the equilibrium rate of $CaCO_3$ dissolution (given mean wt% $CaCO_3$, bottom-water [O_2], organic carbon rain rate, seafloor depth, carbonate chemistry, etc.). Compared to *Archer* [1991], we propagate K_1, K_2, and $K_{sp,cal}$ from the main cGENIE carbonate chemistry solver, allowing us to hence also propagate a Mg/Ca correction. The profiles of porosity and bioturbation rate in the original model are substituted with those of *Ridgwell* [2001]. Here (in comparison to e.g., *Ridgwell and Hargreaves* [2007]), because the model of *Archer* [1991] is an 'oxic-only' approximation and omits the role of NO_3^- and SO_4^{2-} reduction at the higher organic matter rain fluxes characteristic of continental margins, we limit the calculation of $CaCO_3$ dissolution (and hence burial) to depths greater than 1000 m and assume no carbonate preservation at shallower depths. Finally, the numerical solution for steady-state $CaCO_3$ dissolution is not unconditionally stable. In the very few (<1%) model sediment grid points where a robust solution is not achieved, we substitute the explicit scheme with the lookup table of *Ridgwell et al.* [2003] and mask out those particular grid points results (Fig. 4, SI.4 and SI.6).

2.4 Methodology for the carbonate chemistry and steady-state marine carbon cycling evaluation of cGENIE.cookie

We create a 'clean' model comparison where the only differences that can occur in marine carbon cycling and carbonate geochemistry can be due to changing the carbonate dissolution constant and/or Mg/Ca correction schemes. We do this by (a) taking the non-seasonal ocean-atmosphere-only preindustrial (278 pm pCO_2) configuration of *Ridgwell et al.* [2007] so as to minimize any difference between climate states for the same imposed value of atmosphere pCO_2 (which can arise in the seasonal model configuration of *Cao et al.* [2009] as a result of highly non-linear interactions between seasonal sea-ice extent and local ocean-atmosphere climate state), and (b) impose a fixed (annual mean) pattern of $CaCO_3$:POC export rain ratio derived from *Ridgwell et al.* [2007a] to remove feedbacks on carbonate chemistry arising from a response of $CaCO_3$ export to carbonate saturation, (e.g., as per *Ridgwell et al.* [2007b, 2009]). This configuration was run for 10,000

https://doi.org/10.5194/egusphere-2025-5564
Preprint. Discussion started: 10 February 2026

years to equilibrium, using: (A) the default set of carbonate constants (*Mehrbach et al.* [1973]) in cGENIE plus *Ben-Yaakov and Goldhaber* [1973] and *Tyrell and Zeebe* (2004) Mg/Ca correction scheme – the current cGENIE model default, (B) the new carbonate system corrections based on MyAMI (Hain et al. [2015]) which are calibrated to the total *p*H scale (*Dickson and Millero* [1987]) and then converted to seawater *p*H scale assuming internally consistent modern seawater $[SO_4^{2-}]_T$ and $[F^-]_T$ total concentrations, and (C) the default carbonate constant set (*Mehrbach et al.* [1973]) in cGENIE but no Mg/Ca correction scheme. These three experiments were run under major ion concentration assumptions representing both modern ($[Ca^{2+}]$ = 10.2 mmol/kg, mean $[Mg^{2+}]$ = 52.8 mmol/kg) and idealized early Eocene ($[Ca^{2+}]$ = 20.0 mmol/kg, mean $[Mg^{2+}]$ = 30.0 mmol/kg, the same as in Hain et al. [2015]). These experiment combinations are summarized in Table 1. In order to explore parameter space in making the comparisons we take advantage of the fact that a single model experiment provides an array of combinations of environmental (T, S) conditions – a total of 934 surface grid cells with varying permutations of T and S spanning ~-2-37ºC and ~33-39 PSU, respectively.

Table 1: Summary of our simulation ensemble.

Major ion concentration (mmol/kg)	Carbonate system parameter set and Mg/Ca correction scheme	Sediment module and weathering	Experiment identifier	Run duration
'PI-like' (PI) $[Mg^{2+}]$ = 53 $[Ca^{2+}]$ = 10	(A) cGENIE default correction	Off ('OCEAN')	PI-A-ocean	10 kyr
		On with balancing weathering flux ('CLOSED')	PI-A-closed	20 kyr
		On with prescribed weathering ('OPEN')	PI-A-open	100 kyr
	(B) MyAMI lookup	Off	PI-B-ocean	10 kyr
		On, balanced	PI-B-closed	20 kyr
		On, prescribed	PI-B-open	100 kyr
	(B2) MyAMI lookup with temperature limits of cGENIE default	Off	PI-B2-ocean	10 kyr
	(C) cGENIE without Mg/Ca correction	On, balanced	PI-C-closed	20 kyr
		On, prescribed	PI-C-open	100 kyr
'Early Eocene-like' (EE) $[Mg^{2+}]$ = 30 $[Ca^{2+}]$ = 20	(A) cGENIE default	On, balanced	EE-A-closed	20 kyr
		On, prescribed	EE-A-open	100 kyr
	(B) MyAMI lookup	Off	EE-B-ocean	10 kyr
		On, balanced	EE-B-closed	20 kyr
		On, prescribed	EE-B-open	100 kyr
	(C) cGENIE without Mg/Ca correction	On, balanced	EE-C-closed	20 kyr
		On, prescribed	EE-C-open	100 kyr

We start our analysis by simply contrasting the equilibrium carbonate constants derived internally in cGENIE by interpolating within the MyAMI-derived look-up tables vs those explicitly calculated by MyAMI under the same

https://doi.org/10.5194/egusphere-2025-5564
Preprint. Discussion started: 10 February 2026

environmental (boundary) conditions. This reveals the error introduced by interpolating from a lookup table rather than directly calculating the equilibrium constants.

In our second main analysis step, we consider the how the dynamic carbon cycle response differs between carbonate chemistry equilibrium constant correction schemes (default, MyAMI). We are interested in the dynamic redistribution of carbon within the "ocean-atmosphere only" surface environment, the resultant net effect on $CaCO_3$ burial fluxes and hence carbon and alkalinity inventories. To explore this, we set up the model with three different assumptions of Mg/Ca correction scheme (A, B, C; described above and in Table 1), and in three different configurations of ocean-atmosphere-sediment carbon cycling: 'ocean', 'closed' and 'open'. The 'ocean' configuration is an ocean-atmosphere only system with atmospheric CO_2 constantly restored to pre-industrial (278 ppm) with complete and instantaneous dissolution and remineralization of biogenic $CaCO_3$ and organic carbon, respectively, occurring at the sea floor (a 'reflective' boundary condition, *Hülse et al.* [2017]). In this configuration, we are able to assess the direct effect of Mg/Ca corrections on the dissolved carbonate system in a 3D ocean. Next, we configure an ocean-atmosphere-sediment system as per *Ridgwell and Hargreaves* [2007]. This is the same non-seasonally-forced ocean configuration as *Ridgwell et al.* [2007a], and with the imposition of the same fixed spatial field of $CaCO_3$:POC as before. However, instead of dissolving all $CaCO_3$ that reaches the ocean-sediment interface, $CaCO_3$ now enters the upper sediment layers and is dissolved *in situ* or buried depending on local porewater chemistry and calculated by the 1D reaction-transport model of *Archer* [1991]. Loss from the ocean of DIC, ALK, and Ca^{2+} through $CaCO_3$ burial is balanced by an equally input flux of Ca^{2+}, DIC and ALK into the surface ocean. The result is that the total ocean inventories of ALK and Ca^{2+} do not change ('closed' configuration) although CO_2 can independently exchange with the atmosphere depending on the state of the biological pump. In this configuration, we assess the impact of carbonate chemistry scheme and correction on $CaCO_3$ deposition and burial. In the real Earth system, marine inputs would not instantly adjust to changes in marine burial but rather the marine carbonate system would adjust to re-equilibrate marine burial and inputs (the carbonate compensation feedback – e.g., *Ridgwell and Zeebe* [2005]). We assess this full system response by configuring the model as an 'open' system where solute input (from weathering) is fixed and ocean chemistry and $CaCO_3$ burial dynamically adjusts to balance the input flux. We set the fixed input flux of dissolved $CaCO_3$ to $10x10^{12}$ mol C/yr and hence close to modern open ocean burial [*Ridgwell and Hargreaves*, 2007]. Note that in the 'closed' and 'open' configurations, we deviate from *Ridgwell and Hargreaves* [2007] by substituting the 1D reaction-transport model of *Archer et al.* [2000] in place of the original sediment dissolution look-up tables (see Section 2.3). Finally, we apply both modern and an Eocene-like Mg/Ca to all combinations of carbonate chemistry scheme and ocean/closed/open configuration for a total of 3×3×2 (18) permutations of experiments. Of these, we list in Table 1 the subset of 12 permutations that we focus on in the Results, plus one simulation (PI-B2-ocean) testing the importance of user-set temperature limits for the simulated carbonate system.

In summary, we devised and ran an ensemble of model experiments with differing carbonate chemistry scheme, ocean/closed/open configuration, and ocean Mg/Ca to investigate (a) the importance of correcting equilibrium constants for changing ocean $[Ca^{2+}]$ and $[Mg^{2+}]$ (e.g., see: *Ridgwell* [2005], *Zeebe and Tyrrell* [2004]), and (b) what the implications are for the global carbon cycle of the Mg/Ca correction assumption as well as the importance of changes in bulk ocean $[Ca^{2+}]$.

https://doi.org/10.5194/egusphere-2025-5564
Preprint. Discussion started: 10 February 2026

3. Results and Discussion

We start presentation and discussion of our results with an assessment of the accuracy of our lookup-table implementation of MyAMI-derived interpolated *K* values (Section 3.1), followed by an evaluation of the impacts on the carbonate system parameters and marine carbon cycling of changing from the default set of carbonate constants to the MyAMI-derived constant set – both experiments conducted under modern (PI) seawater [Mg^{2+}] and [Ca^{2+}] and hence implicitly with no Mg/Ca correction being applied (Section 3.2). In Section 3.3 under assumed Early Eocene (EE) seawater [Mg^{2+}] and [Ca^{2+}] conditions we then assess the implications for ocean carbonate chemistry as well as $CaCO_3$ preservation and burial in marine sediments, of applying the default cGENIE and MyAMI-derived Mg/Ca correction schemes and vs. no applied correction. We end with a discussion of the implications for the interpretation and data assimilation of paleoenvironmental proxies (Section 3.4).

3.1 Evaluation of the interpolated lookup approximation of MyAMI carbonate constant characteristics.

https://doi.org/10.5194/egusphere-2025-5564
Preprint. Discussion started: 10 February 2026

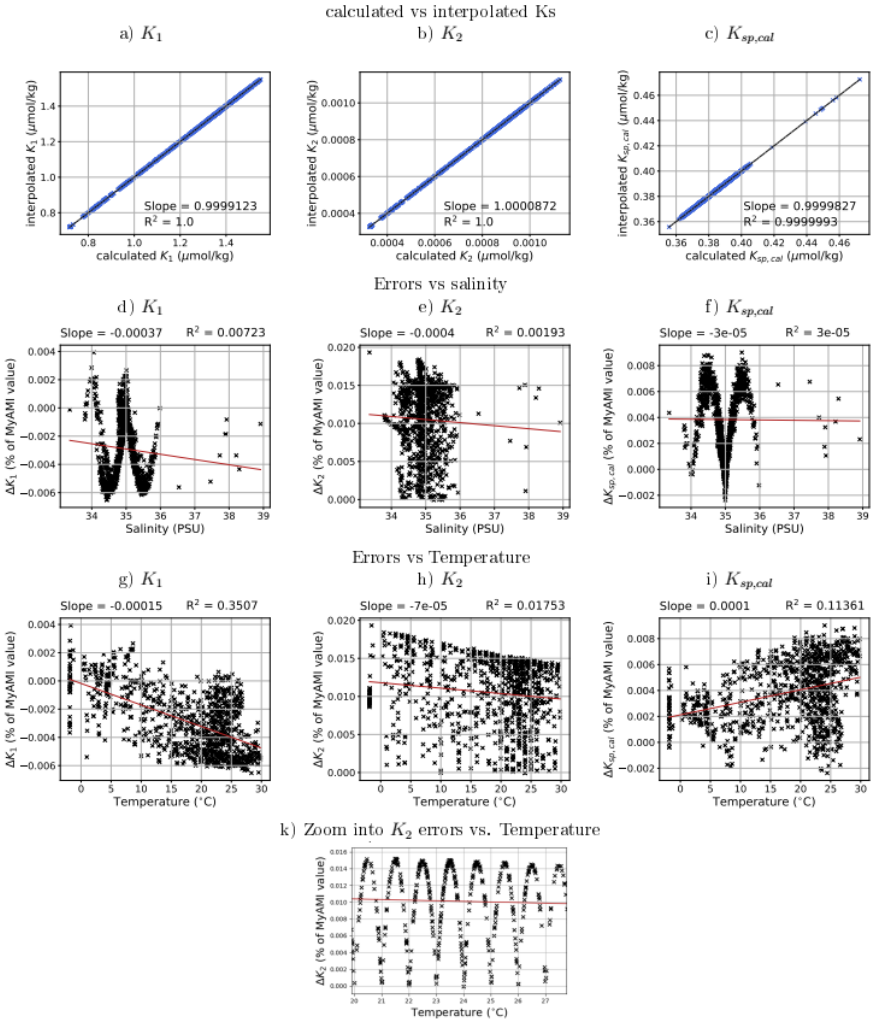

Figure 2: Errors due to interpolating rather than calculating *in situ* K_1 in the surface ocean in simulation EE-B-ocean. All errors are given as percentage of the exact MyAMI value.

The values of K_1, K_2 and $K_{sp,cal}$ calculated directly using MyAMI are compared with the internal cGENIE interpolation in each of the model surface ocean grid cells (934 points), for the specific combination of T, S, $[Mg^{2+}]$, and $[Ca^{2+}]$ of simulation EE-B-ocean with Early Eocene-like Mg/Ca (Fig. 2). The differences are vanishingly small (~0.02 % at most) and two to three orders of magnitude smaller than their respective spatial variability. We find that the interpolation errors are smaller than the precision of MyAMI (Hain et al. [2015]) and the empirical uncertainty of the constants (Orr et al. [2018]), and thus conclude that the interpolated carbonate constants could not be distinguished from the directly calculated ones in the real world. Still, we analyse the errors to understand how the design of the discrete, evenly sampled look-up table and multi-dimensional linear interpolation affects the carbonate constants applied to cGENIE. At a given combination of T, S, $[Mg^{2+}]$, and $[Ca^{2+}]$ the total error is composed of the errors caused by linear interpolation in each dimension. The largest error is caused by the interpolation that least captures the functionality in the respective dimension, either because that functionality is poorly approximated by a linear fit or because the sampling in that dimension is too

https://doi.org/10.5194/egusphere-2025-5564
Preprint. Discussion started: 10 February 2026

coarse to capture its complexity. For K_1 and $K_{sp,cal}$, the interpolation of the salinity dependence causes the largest errors, evidenced by the sinusoidal distribution of the error on the salinity grid, with the largest errors occurring at half-distance between the sampled salinities (every 1 PSU). This suggests that the coarse sampling in the salinity-space dominates the interpolation error in K_1 and $K_{sp,cal}$. For K_2, instead, the interpolation along the temperature axis creates the largest errors, again distributed sinusoidally (Fig. 2k). The interpolation errors are generally larger for K_2, which is more sensitive to $[Mg^{2+}]$ and $[Ca^{2+}]$ changes than K_1 due to the high complexation potential of the carbonate ion (Hain et al. [2015, 2018]). Overall, this reaffirms our assertion that use of an interpolation method to substitute for the underlying MyAMI code does not introduce substantial errors.

3.2 Impact of changing carbonate system constants (cGENIE default vs. MyAMI-derived).

First, we consider differences induced by using the MyAMI-derived carbonate system parameters instead of the ones calculated based on Mehrbach et al. [1973] (the default parameters in cGENIE) in modern seawater (PI) and with cGENIE configured in an ocean(/atmosphere)-only configuration (PI-B-ocean vs PI-A-ocean). The default equilibrium constants in cGENIE have slightly different temperature and salinity dependencies than those derived by the Pitzer model contained in MyAMI for each local combination of $[Mg^{2+}]$ and $[Ca^{2+}]$. This causes additional and larger differences than those caused by the interpolation despite the pre-industrial carbonate system not needing Mg/Ca corrections, but they are still minimal compared to the spatial variability of these constants. It is worth noting that the small differences between MyAMI-derived constants and Mehrbach et al. constants primarily stem from the fact that MyAMI is calibrated to the standard 'best practice' carbonate equilibrium constants from Dickson et al. [2007]. The Dickson constant set, though originally based on Mehrbach et al.'s measurements, is calibrated to the total *p*H scale and intended for use in modern seawater chemistry. Thus, the shift from the Mehrbach-PI ocean to the MyAMI-PI ocean theoretically improves cGENIE's representation of preindustrial ocean chemistry, making it more directly comparable to empirical measurements that employ Dickson's standard practice *K*s. Though the differences remain quite small, we describe their spatial pattern in the surface ocean to provide a sense of their effect on the simulated carbonate system.

https://doi.org/10.5194/egusphere-2025-5564
Preprint. Discussion started: 10 February 2026

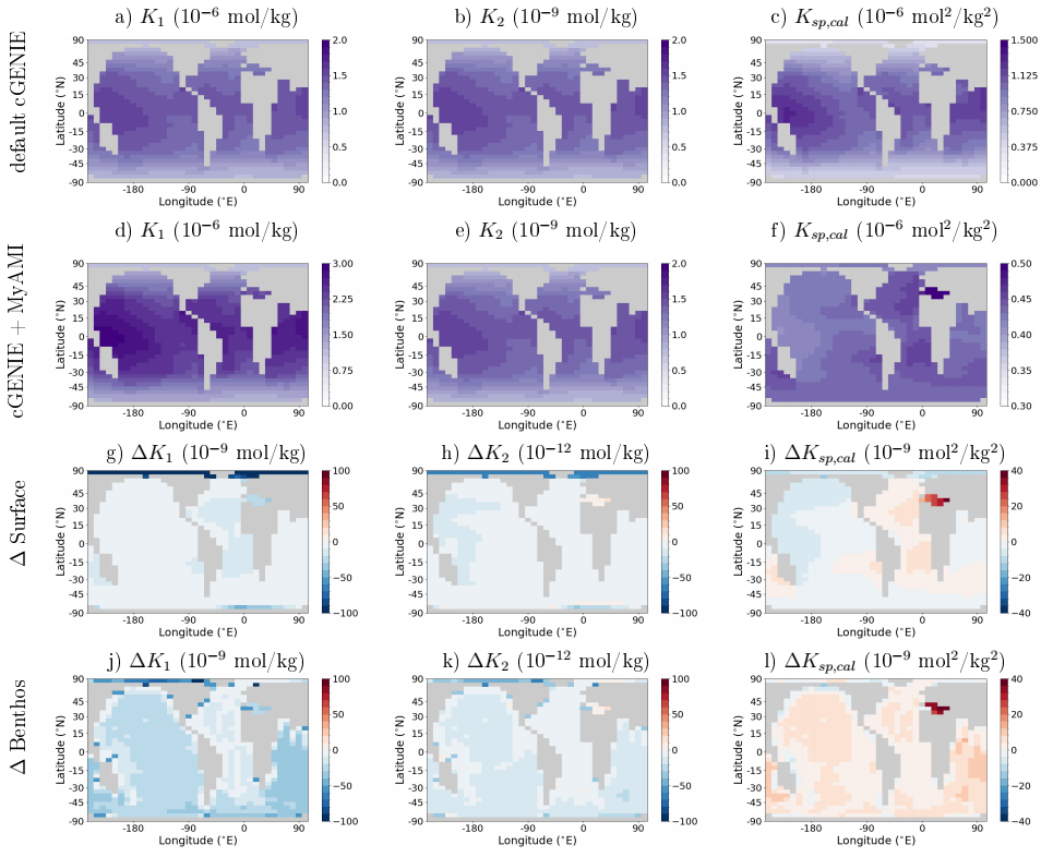

Figure 3: Absolute surface ocean K_1, K_2, and $K_{sp,cal}$ in default cGENIE (PI-A-ocean) and cGENIE+MyAMI (PI-B-ocean) solutions for the pre-industrial carbonate system (a-f) and difference between the two (simulations PI-B-ocean minus PI-A-ocean) for the surface and benthic ocean.

Differences between default and MyAMI-derived *K*s are largest at the margins of the sampled parameter range, particularly in the cold and relatively fresh Arctic and salty Mediterranean (Fig. 3). In the Arctic, K_1, K_2 and K_B are all lower, which reduces [H^+] and thus increases *p*H (Fig. SI.1). These changes cause a reduction in [CO_3^{2-}] and a small increase in [HCO_3^-] despite the lower K_1, which drives a marginal overall DIC increase in Arctic waters. Reductions of $K_{sp,cal}$ coincident with the K_2 changes lessen the impact on Ω, which consequently shows little change. These high-latitude differences are strongly affected by the different temperature limits for the default Mehrbach scheme and the MyAMI-derived constants and are not present when we apply the same temperature limits in both cases (Fig. SI.2). The temperature limits do not affect the rest of the surface ocean as sea-surface temperatures outside the high-latitudes are within the temperature limits of both schemes. Outside the Arctic, MyAMI-derived K_1 is lower across the surface ocean, with the largest differences in the Mediterranean, followed by the Atlantic. The difference in K_2 shows the opposite pattern, with largest decreases in the Western Pacific and an increase in the Mediterranean. Thus, in the Atlantic and Mediterranean the dissociation of carbonic acid is less favourable and the dissociation of [HCO_3^-] remains unchanged or is slightly increased, respectively, resulting in less [HCO_3^-] and more [CO_3^{2-}]. Despite increased [CO_3^{2-}], Ω is lower in Mediterranean and Atlantic surface waters because of a higher $K_{sp,cal}$. In the Western Pacific, the K_2 decrease outcompetes the effect of reduced K_1, like in the Arctic, and thus leads to increased [HCO_3^-] and reduced [CO_3^{2-}]. These carbon speciation anomalies

https://doi.org/10.5194/egusphere-2025-5564
Preprint. Discussion started: 10 February 2026

in the surface Atlantic are advected into the deep Atlantic with the meridional overturning circulation. In the deep Atlantic a small Ω increase is largely due to the $[CO_3^{2-}]$ decrease and, to a lesser extent, the increased $K_{sp,cal}$, while in most of the benthic Indo-Pacific the $K_{sp,cal}$ change dominates and slightly reduces Ω.

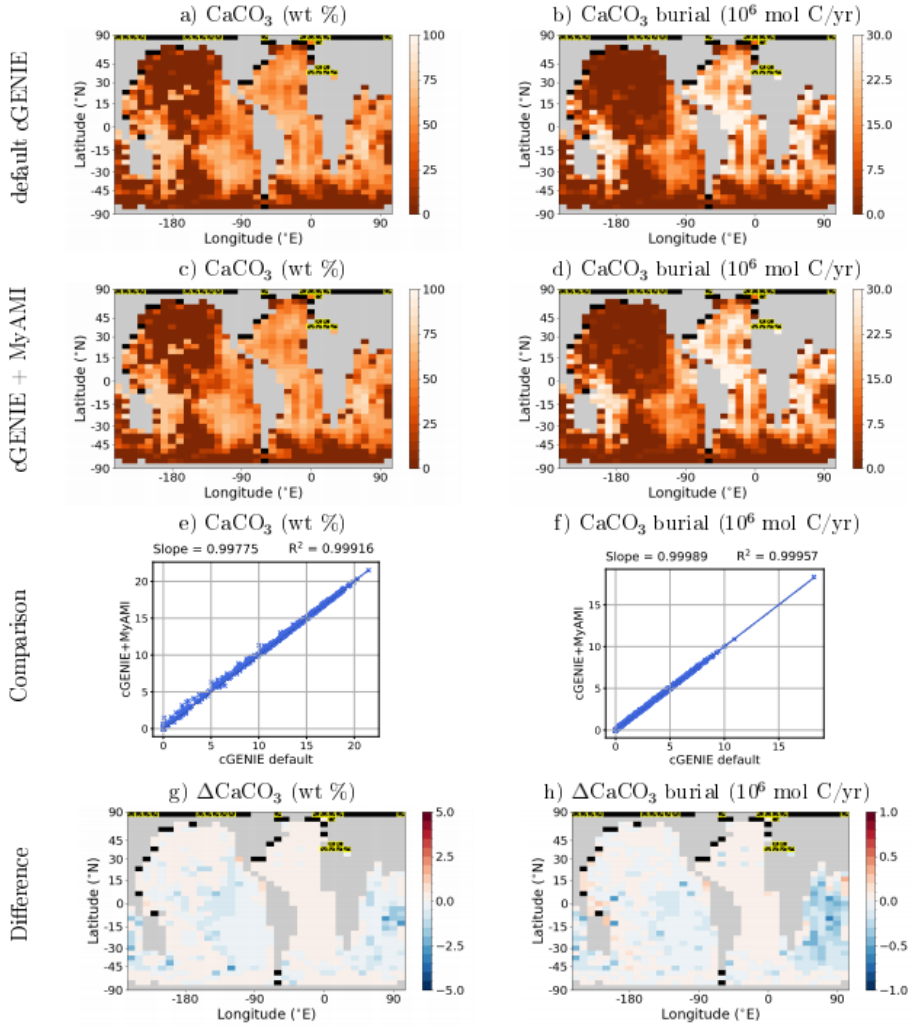

Figure 4: Absolute distributions and differences in the carbonate content in surface sediments and burial rates with the default scheme (simulation PI-A-open) and cGENIE+MyAMI (PI-B-open) for pre-industrial Mg/Ca. Sediments shallower than 1000 m are masked in black and locations where the sedimentary carbonate system could not be solved dynamically and was instead replaced by a lookup table value is hatched in yellow.

When we include marine sediments in our model configuration (PI-B-closed vs. PI-A-closed), any changes made to the marine carbonate system constants are entrained into the sediment module. The benthic Ω decrease across most of the Indo-Pacific leads to a small reduction of $CaCO_3$ accumulation, and ultimately burial, in sediments (Fig. 4). In the Atlantic, Ω is increased slightly despite the $K_{sp,cal}$ change because it is overcompensated by the increased CO_3^{2-}, resulting in increased $CaCO_3$ preservation. In a fully open system (PI-B-open vs PI-A-open), the changed carbonate preservation

https://doi.org/10.5194/egusphere-2025-5564
Preprint. Discussion started: 10 February 2026

pattern alters the flux of DIC, calcium and alkalinity back into the ocean, which shifts the marine carbonate system until total burial fluxes are re-equilibrated with the terrestrial ALK and DIC supply, which in our setup remains constant. These feedback relationships constitute the "carbonate compensation" dynamic of the open system carbon cycle (Hain et al. [2025]). In the case of modern seawater (PI), these shifts are small in the global average. Total DIC in the ocean is 24 PgC higher and mean weight percent of carbonate in surface sediments is -0.12 % lower with the MyAMI-derived *K*s in the open system. Locally, the differences can be slightly higher, especially in the transitory depth zone between full carbonate preservation and full carbonate dissolution, resulting in slightly increased burial in the Indian Ocean and open Pacific, decreased burial rates in the Atlantic, and altered sediment composition in a few isolated grid cells (Fig. 4).

3.3 Implications of applying Mg/Ca carbonate system corrections for Early Eocene-like seawater composition

In the cGENIE model, a change in seawater major ion composition (here: $[Ca^{2+}]$ and $[Mg^{2+}]$) has three distinct effects on seawater carbon chemistry and the global carbon cycle: (1) the saturation (Ω) of $CaCO_3$ changes proportionally with seawater $[Ca^{2+}]$ (e.g., *Ridgwell* [2005]), (2) the equilibrium constants respond with modest changes due to weak specific ion-ion interactions, affecting the equilibrium carbonate speciation between CO_2, bicarbonate, and carbonate ion and shifting *p*H, and (3) the degree of carbonate ion complexation decreases due to the reduced total of divalent cations, as formulated by Millero and Pierrot [1998] and implemented in MyAMI (Hain et al. [2015, 2018]). In a closed system (without any addition or removal of carbon or alkalinity from the model) theimpacts on carbonate speciation and $CaCO_3$ saturation are realized instantaneously in response to a change in seawater composition. However, changes in CO_2 and Ω include carbon cycle feedbacks (Hain et al. [2024]) and to re-balance weathering on land and $CaCO_3$ burial in the ocean (an open system), the global carbon and alkalinity inventories will adjust. Here we assess these three main effects in the context of both closed and open system and all under seawater Mg/Ca representative of the Early Eocene.

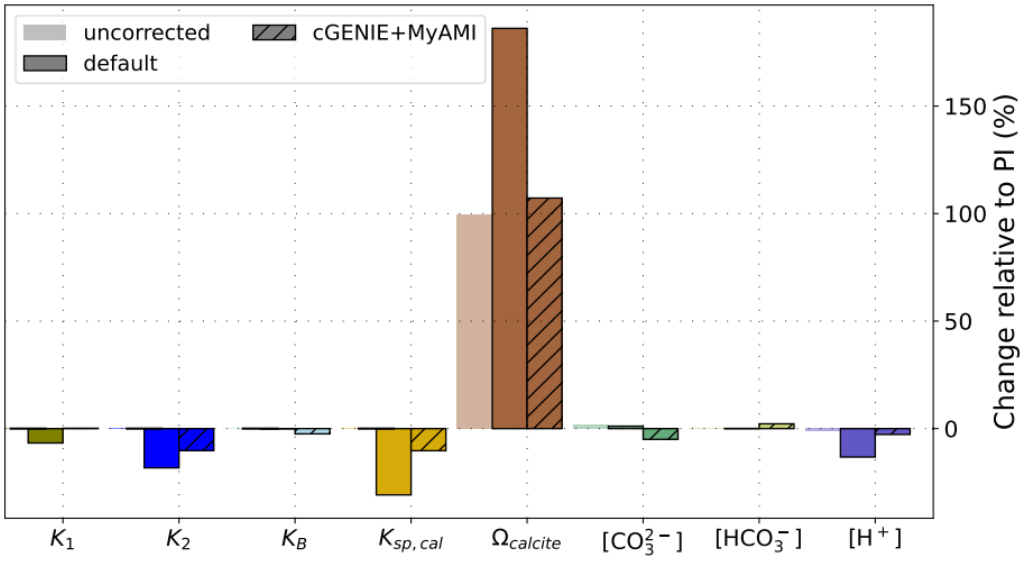

Figure 5: Changes of the global mean surface values of selected dissociation constants and carbonate system metrics due to changing $[Mg^{2+}]$ and $[Ca^{2+}]$ from pre-industrial to Early Eocene-like in simulations without corrections (simulations

https://doi.org/10.5194/egusphere-2025-5564
Preprint. Discussion started: 10 February 2026

EE-C-closed minus PI-C-closed, on the left side of each set of bars) default cGENIE correction (simulations EE-A-closed minus PI-A-closed, middle bar in each set) and cGENIE+MyAMI (EE-B-closed minus PI-B-closed, on the right side of each pair of bars). The changes are given as percentage of the PI values.

The impact of changing seawater major ion composition in a closed system under default (EE-A-closed), MyAMI-based (EE-B-closed), and no Mg/Ca correction (EE-C-closed) are shown in Fig. 5. Ignoring for now the response of Ω (discussed later), of the three effects we find that the complexation of carbonate is the most significant. This is because the calcium and magnesium concentration changes effectively reduce divalent cation concentration by about 20%, thereby significantly increasing the activity coefficient of total carbonate ion and reducing K_2. For example, at modern surface DIC/ALK the decrease in carbonate complexation effectively raises *p*H and repartitions alkalinity from carbonate ion to borate ion, driving 5-10 % reductions in total carbonate ion, CO_2 and $[H^+]_{total}$ and corresponding increases in bicarbonate (Fig. 5) and borate. The differences between the *K*s in the uncorrected cGENIE simulation (EE-C-closed) and those in the cGENIE+MyAMI simulation (EE-B-closed) also vary spatially, with the largest K_1 differences in cold waters of the deep ocean and polar surface oceans, the largest K_2 differences in the warm tropical surface waters and the largest $K_{sp,cal}$ differences in the deep ocean (Fig. 6).

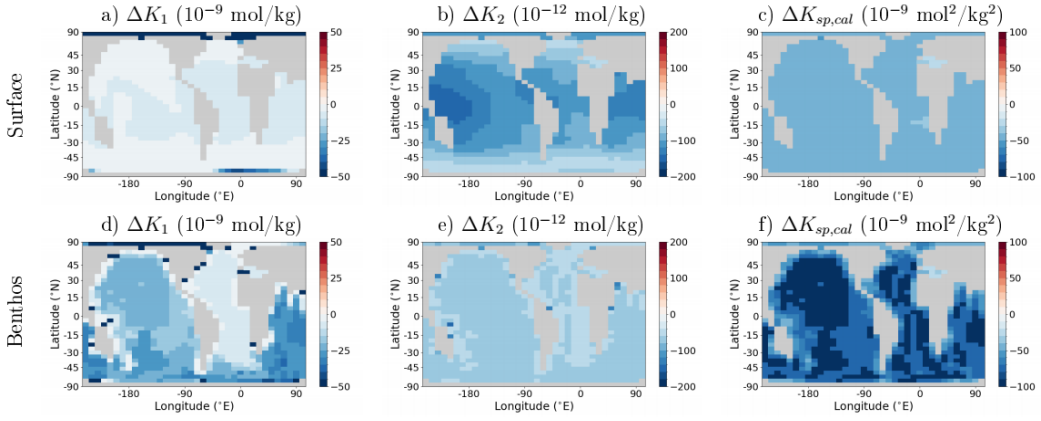

Figure 6: Differences in K_1, K_2, and $K_{sp,cal}$ between uncorrected cGENIE and cGENIE+MyAMI solutions for the carbonate system of the surface and benthic ocean with Eocene-like Mg/Ca (simulations EE-B-closed minus EE-C-closed).

Because the magnitude of the equilibrium constant corrections is significant for Eocene seawater, the choice of correction scheme also becomes relevant. Hain et al. [2015] showed that the equilibrium constants adjusted with MyAMI differ from those adjusted with the cGENIE default schemes, especially for large deviations from PI conditions, because of different sensitivities to $[Ca^{2+}]$ and $[Mg^{2+}]$. Specifically, K_1, K_2 and $K_{sp,cal}$ decrease more (PI to EE) with the standard corrections than with those calculated by MyAMI (Fig. 5; Fig. 2 of Hain et al. [2015]). The coincident change in $[Ca^{2+}]$ and $[Mg^{2+}]$ only causes a minor (2%) decrease in K_1 with MyAMI, suggesting that the changes of hydrogen ion and bicarbonate ion activity almost cancel out. Carbonate ion activity, however, is sensitive to changing ionic strength (e.g., Garrels & Thompson [1962]; Pytkowicz & Hawley [1974]). Any reduction in the total divalent cation concentration of seawater – as in the change from modern to Eocene – will tend to reduce the fraction of total carbonate ion that is complexed into stable ion-pairs with the divalent cations. That is, in modern seawater 36% of total carbonate ion molecules are free (64%

https://doi.org/10.5194/egusphere-2025-5564
Preprint. Discussion started: 10 February 2026

complexed), and with the lower Eocene total divalent cation concentration 39.5% of total carbonate ion molecules are free - corresponding to a ~10% increase in the total carbonate ion activity coefficient, and hence a decrease in K_2. Carbonate ion activity also dominates the response of the $CaCO_3$ solubility constants $K_{sp,cal}$, and both K_2 and $K_{sp,cal}$ need to decrease by the same amount to account for changes in carbonate complexation, as is the case for MyAMI (Hain et al. [2015]) but in contrast to the combination of $K_{sp,cal}$ of Tyrrell and Zeebe [2004] and K_2 of Ben-Yaakov and Goldhaber [1973].

When considering the effects of changing speciation and seawater major ion composition on the $CaCO_3$ saturation index Ω there are additional factors to consider. In approximately doubling Eocene seawater $[Ca^{2+}]$ relative to modern and in the absence of any change in the concentration of total carbonate ion, we would expect Ω would increase proportionately. Indeed, for no applied Mg/Ca correction and virtually no change in $K_{sp,cal}$ or $[CO_3^{2-}]$ (which in any case largely cancel out – see E28), this is what we observe in the model (+98%, Fig. 5). Including a Mg/Ca correction modifies this response. With the MyAMI-based carbonate constants, there is an additional +10% increase in Ω due to reduced carbonate complexation (at constant total carbonate ion), which, coupled with a 7% decrease resulting from the simulated total carbonate ion decline, gives a total 103% increase in Ω in our simulations (Fig. 5). In contrast, with the $K_{sp,cal}$ correction factor of Tyrrell and Zeebe [2004] previously implemented in cGENIE (e.g., Panchuk et al. [2008]) the Ω increase is ~2.7-fold (+170 %), or about two thirds greater than computed with MyAMI (Hain et al. [2015], Fig. 5), and with only a small portion of this attributable to the difference in $[CO_3^{2-}]$ decrease. Hence, using the Tyrrell and Zeebe [2004] correction factor for the $CaCO_3$ solubility constants $K_{sp,cal}$ may lead to significant biases compared to the use of MyAMI which explicitly includes carbonate complexation by divalent cations.

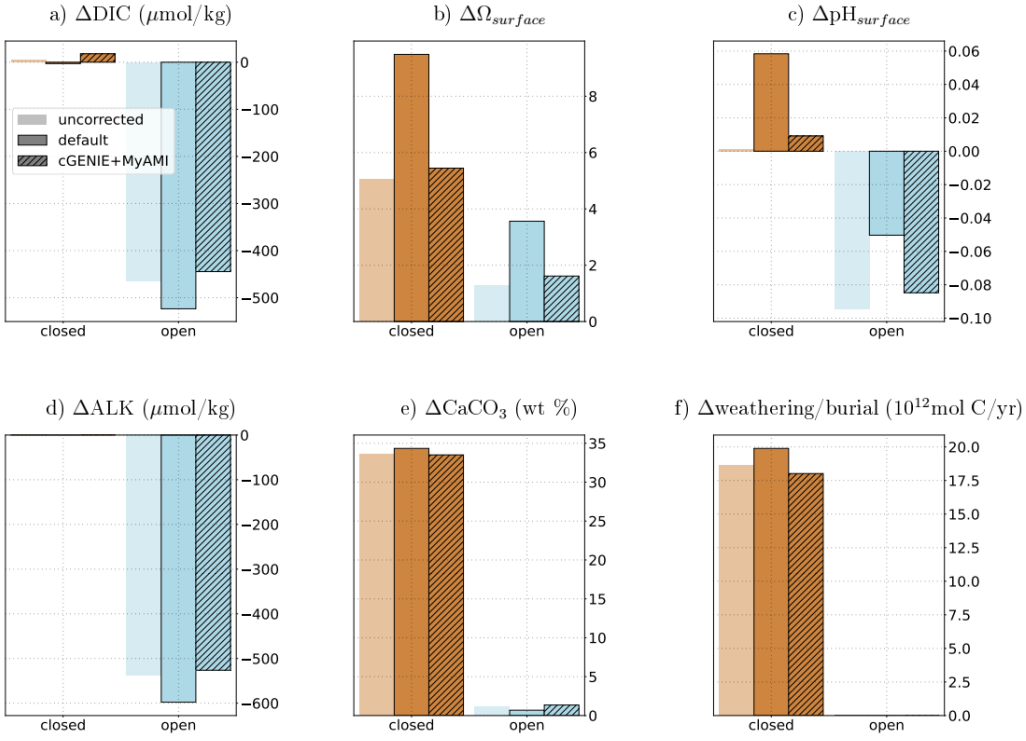

Figure 7: Effect of changing Mg/Ca from pre-industrial to Eocene-like for mean ocean DIC and ALK changes, mean

https://doi.org/10.5194/egusphere-2025-5564
Preprint. Discussion started: 10 February 2026

surface *p*H and Ω, average $CaCO_3$ content of marine sediments and total $CaCO_3$ burial in simulations without correcting for major ion changes, default cGENIE and cGENIE+MyAMI.

In our closed system configuration, simulated Ω changes drive very large increases in $CaCO_3$ preservation (reflected in core-top wt% $CaCO_3$) and hence burial (Fig. 7), with the global sediment accumulation rate of $CaCO_3$ increasing disproportionately in response to Ω – from 9.0 Tmol yr^{-1} (PI, no correction) to 27.6 Tmol yr^{-1}. Because the $[Ca^{2+}]$ effect on Ω is dominant (see above) we find that the different Mg/Ca correction schemes exert only a relatively minor modulation of $CaCO_3$ wt% and burial. In the closed system experiments, carbonate system changes cause small shifts in marine carbon storage, with a ~13 µmol/kg mean ocean DIC loss in default cGENIE but a ~18 µmol/kg mean ocean DIC gain in cGENIE+MyAMI because the applied restoring of the atmospheric CO_2 concentration allows for net C loss or gain in the atmosphere-ocean system at constant ALK.

Finally, setting up cGENIE model experiments with a constant global terrestrial weathering rate (and hence invariant fluxes of DIC and ALK) in an 'open' system configuration, the initial imbalance in (enhanced) $CaCO_3$ burial vs. (fixed) weathering drives the DIC and ALK composition of the ocean lower and away from that of the closed system. Once the system has re-balanced with $CaCO_3$ burial equal to weathering (we run our experiments for 100 kyr to achieve this), DIC, ALK, and *p*H are all lower than was the case for PI $[Ca^{2+}]$ and $[Mg^{2+}]$, while Ω is slightly higher. For no applied Mg/Ca correction and hence a purely $[Ca^{2+}]$ induced reorganization of marine carbon cycling (EE-C-open), the changes are respectively: -465 µmol/kg DIC and -538 µmol/kg ALK (on a mean global ocean), -0.094 *p*H units and +1.28 Ω (on a global ocean surface mean basis). When applying the MyAMI-based Mg/Ca correction (EE-B-open), we find that the decreases in DIC and ALK are slightly reduced (by 20 µmol/kg and 12 µmol/kg, respectively), Fig. 7), resulting in a slightly greater increase in Ω but smaller decline in *p*H. In contrast, the default cGENIE Mg/Ca correction scheme (EE-A-open) results in the carbonate saturation increase almost being doubled, and the *p*H decrease halved – differences that largely occur because K_1, K_2 and $K_{sp,cal}$ decrease less when corrected with MyAMI rather than the default scheme (Fig. 5). Spatially, differences between correction schemes appear across the whole non-Arctic surface ocean and are largest in warm waters for K_1 and K_2 and saltier waters for $K_{sp,cal}$ (Fig. SI.3). Consequently, *p*H is 0.04-0.06 lower and Ω higher across most of the surface ocean when the MyAMI rather than the default scheme is used in our simulations (Fig. SI.4).

3.4 Implications for interpreting paleoenvironmental proxies

By updating the simulated carbonate system in cGENIE, the MyAMI-derived constants also correct the representation of model variables that can be directly compared to paleoenvironmental proxies. Examples are the $CaCO_3$ fraction of marine sediments and marine $CaCO_3$ burial, which have been used to constrain past marine carbonate system states (e.g. Si et al. [2023], Li et al. [2024]). For Eocene-like $[Mg^{2+}]$ and $[Ca^{2+}]$, simulated $CaCO_3$ fraction of marine sediments and marine $CaCO_3$ burial are slightly different with MyAMI-derived constants (simulation EE-B-open) than with the default correction scheme (simulation EE-A-open, Fig. SI.4 e-f, SI.5 e-f) due to the discussed changes in deep ocean Ω, highlighting the potential for a small error in model-data comparisons without the new scheme.

In addition to correcting the representation of major ion effects on marine carbon cycling, the new carbonate system correction also enables a more direct comparison of simulated and reconstructed *p*H (when both are reported on the total

https://doi.org/10.5194/egusphere-2025-5564
Preprint. Discussion started: 10 February 2026

scale). This is because the Mg/Ca correction of B alkalinity adds to the differences of surface ocean carbonate system solutions between MyAMI and the default cGENIE carbonate system. We demonstrate this by comparing the marine dissolved boron (B) reservoir that is simulated in cGENIE with the default vs. new MyAMI-derived scheme.

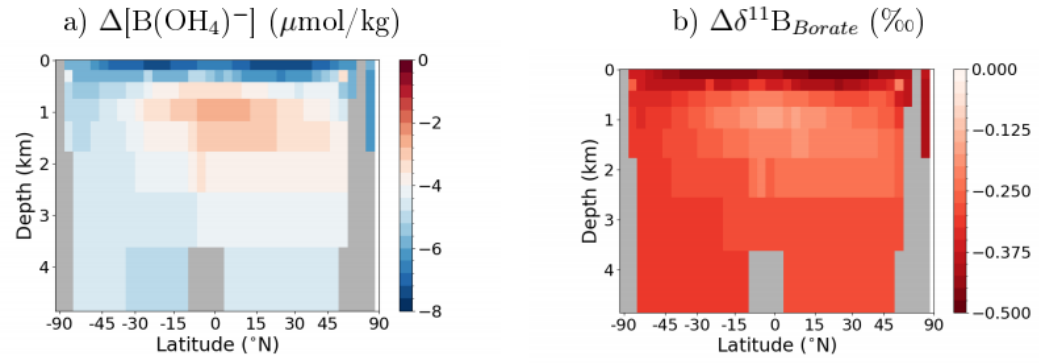

Figure 8: Zonally-averaged profiles of differences in borate ion concentrations and $\delta^{11}B$ of borate derived from K_B and *p*H between cGENIE+MyAMI and default cGENIE (simulations EE-B-open minus EE-A-open) for the Pacific.

cGENIE accounts for borate concentrations in the total alkalinity, but the dissociation constant for boric acid K_B is not corrected for Mg/Ca in the default scheme. The new scheme imports K_B for local conditions from MyAMI. In our simulation EE-B-open, this leads to a slightly lower surface K_B in the global average than under PI conditions (Fig. 5), and hence the carbonate system is solved with lower borate ion concentrations than in simulation EE-A-open with the default scheme. Fig. 8 shows that the borate concentration differences are highest in the surface ocean where they reach up to -12 µmol/kg.

Assuming modern-day $\delta^{11}B$ of seawater (39.61 ‰) and a α value of 1.0272 (Klochko et al. [2006]), we estimate $\delta^{11}B$ of borate from the difference between pK_B and *p*H (Fig. 8):

$$\delta^{11}B_{Borate} = (39.61‰ \times (1.0 + 10^{pK_B\text{-}pH}) - 27.2 \times 10^{pK_B\text{-}pH}) \; / \; (1.0 + \alpha \times 10^{pK_B\text{-}pH})$$

The differences in the local dissociation constants for boric acid translate into differences of up to 0.5 ‰ in the $\delta^{11}B$ of borate ions in the surface ocean, corresponding to up to 0.04 *p*H units. This highlights the relevance of Mg/Ca corrections for B-based *p*H estimates and shows how internal inconsistencies can arise when different Mg/Ca corrections are used in comparisons of local *p*H reconstructions and simulated carbonate systems in Earth system models.

Conclusions

We implemented a new carbonate chemistry scheme in cGENIE.cookie to correct the simulated carbonate system equilibria based on the MyAMI model via look-up tables. We evaluated the accuracy of the scheme by comparing our interpolated carbonate system parameters to those directly calculated with MyAMI. We then assessed the effects of the new scheme on the simulated carbonate system in cGENIE. Using MyAMI-derived carbonate system parameters introduces small differences in the simulated pre-industrial carbonate system. When simulating a carbonate system which requires ion-pairing corrections, in our case by changing marine $[Ca^{2+}]$ and $[Mg^{2+}]$ to Early Eocene-like values, the new

https://doi.org/10.5194/egusphere-2025-5564
Preprint. Discussion started: 10 February 2026

scheme results in lower surface ocean saturation state and *p*H increases than the default scheme in a closed system and less ALK and DIC loss and a larger surface ocean *p*H decline in an open system than the default scheme. These differences demonstrate the importance of updating the default cGENIE carbonate system corrections for major ion concentrations and exemplify the systematic bias that exists when comparing the carbonate system simulated with cGENIE's default scheme to observations.

Acknowledgements

MA and SEG acknowledge financial support from NERC Grant NE/P01903X/. SEG and AR acknowledge financial support from NERC Grant NE/W009625/1.
MPH and TG acknowledge discussion with part of the IAPWS/SCOR/IAPSO-JCS marine chemical speciation task group.
MJH and MA acknowledge financial support from UKRI Frontier Research Guarantee Grant EP/X025918/1.
AR acknowledges financial support from National Science Foundation grants EAR-2121165 and OCE-2244897.

Code and data availability

The code for the version of the 'cookie' release of the cGENIE Earth system model used in this paper, is tagged as v0.9.90, and is assigned a DOI: 10.5281/zenodo.17537316 (Ridgwell et al. [2025]).
The branch used to generate the model expeirments is: main.DEV
Configuration files for the specific experiments presented in the paper can be found in the directory: genie-userconfigs/PUBS/submitted/Adloff_et_al.GMDD.2025. Details of the experiments, plus the command line needed to run each one, are given in the readme.txt file in that directory. All other configuration files and boundary conditions are provided as part of the code release.
A manual detailing code installation, basic model configuration, tutorials covering various aspects of model configuration, experimental design, and output, plus the processing of results, is assigned a DOI: 10.5281/zenodo.17537474 (Ridgwell [2025]).

Author contributions

AR, SEG, MPH and MJH conceptualised the model development. SEG secured funding for the model development. MA produced and implemented the lookup tables of MyAMI-derived equilibrium constants. AR made additional adjustments to the cGENIE code base and ran the final set of experiments. MA, AR and SEG analysed the results, which were discussed with all authors. MA, TG, MPH and AR wrote the manuscript draft and all authors contributed to the final version.

https://doi.org/10.5194/egusphere-2025-5564
Preprint. Discussion started: 10 February 2026

References

Anagnostou, E., John, E.H., Babila, T.L., Sexton, P.F., Ridgwell, A., Lunt, D.J., Pearson, P.N., Chalk, T.B., Pancost, R.D. and Foster, G.L., 2020. Proxy evidence for state-dependence of climate sensitivity in the Eocene greenhouse. *Nature communications*, *11*(1), pp.1-9.

Ben-Yaakov, S. and Goldhaber, M.B., 1973, January. The influence of sea water composition on the apparent constants of the carbonate system. In *Deep Sea Research and Oceanographic Abstracts* (Vol. 20, No. 1, pp. 87-99). Elsevier.

Berner, R.A., 1975. The role of magnesium in the crystal growth of calcite and aragonite from sea water. *Geochimica et Cosmochimica Acta*, *39*(4), pp.489-504.

Branson, O., Whiteford, R., Filipe, & Coenen, D. ,2023. Oscarbranson/cbsyst: 0.4.9 - Zenodo. doi: 10.5281/zenodo.1402261

Brennan, S.T., Lowenstein, T.K. and Cendón, D.I., 2013. The major-ion composition of Cenozoic seawater: The past 36 million years from fluid inclusions in marine halite. *American Journal of Science*, *313*(8), pp.713-775.

Cao, L., Eby, M., Ridgwell, A., Caldeira, K., Archer, D., Ishida, A., Joos, F., Matsumoto, K., Mikolajewicz, U., Mouchet, A. and Orr, J.C., 2009. The role of ocean transport in the uptake of anthropogenic CO 2. *Biogeosciences*, *6*(3), pp.375-390.

Cenozoic CO2 Proxy Integration Project (CenCO2PIP) Consortium, Hönisch, B., Royer, D.L., Breecker, D.O., Polissar, P.J., Bowen, G.J., Henehan, M.J., Cui, Y., Steinthorsdottir, M., McElwain, J.C. and Kohn, M.J., 2023. Toward a Cenozoic history of atmospheric CO2. Science, 382(6675), p.eadi5177.

Clegg, S.L., Waters, J.F., Turner, D.R. and Dickson, A.G., 2023. Chemical speciation models based upon the Pitzer activity coefficient equations, including the propagation of uncertainties. III. Seawater from the freezing point to 45° C, including acid-base equilibria. Marine Chemistry, 250, p.104196.

Dickson, A.G. and Millero, F.J., 1987. A comparison of the equilibrium constants for the dissociation of carbonic acid in seawater media. *Deep Sea Research Part A. Oceanographic Research Papers*, *34*(10), pp.1733-1743.

Garrels, R.M. and Thompson, M.E., 1962. A chemical model for sea water at 25 degrees C and one atmosphere total pressure. *American Journal of Science*, *260*(1), pp.57-66.

Hain, M.P., Sigman, D.M., Higgins, J.A. and Haug, G.H., 2015. The effects of secular calcium and magnesium concentration changes on the thermodynamics of seawater acid/base chemistry: Implications for Eocene and Cretaceous ocean carbon chemistry and buffering. *Global Biogeochemical Cycles*, *29*(5), pp.517-533.

Hain, M. P., Sigman, D. M., Higgins, J. A. and Haug, G. H., 2018. Response to Comment by Zeebe and Tyrrell on "The Effects of Secular Calcium and Magnesium Concentration Changes on the Thermodynamics of Seawater Acid/Base

https://doi.org/10.5194/egusphere-2025-5564
Preprint. Discussion started: 10 February 2026

Chemistry: Implications for the Eocene and Cretaceous Ocean Carbon Chemistry and Buffering," Glob. Biogeochem. Cyc., 32(5), 898–901, doi:https://doi.org/10.1002/2018GB005931.

Hain, M.P., Allen, K.A. and Turner, S.K., 2024. Earth system carbon cycle dynamics though time. In A. D. Anbar, & D. Weis (Eds.), *Treatise on geochemistry* (3rd ed.). Hardback.

Hardie, L.A., 1996. Secular variation in seawater chemistry: An explanation for the coupled secular variation in the mineralogies of marine limestones and potash evaporites over the past 600 my. *Geology*, *24*(3), pp.279-283.

Harvie, C.E., Møller, N. and Weare, J.H., 1984. The prediction of mineral solubilities in natural waters: The Na-K-Mg-Ca-H-Cl-SO4-OH-HCO3-CO3-CO2-H2O system to high ionic strengths at 25 ˚C. Geochimica et Cosmochimica Acta, 48(4), pp.723-751.

Horita, J., Friedman, T.J., Lazar, B. and Holland, H.D., 1991. The composition of Permian seawater. *Geochimica et Cosmochimica Acta*, *55*(2), pp.417-432.

Hülse, D., Arndt, S., Wilson, J.D., Munhoven, G. and Ridgwell, A., 2017. Understanding the causes and consequences of past marine carbon cycling variability through models. *Earth-Science Reviews*, *171*, pp.349-382.

Hülse, D. and Ridgwell, A., 2025. Instability in the geological regulation of Earth's climate. *Science*, *389*(6767), p.eadh7730. DOI: 10.1126/science.adh7730

Klochko, K., Kaufman, A.J., Yao, W., Byrne, R.H. and Tossell, J.A., 2006. Experimental measurement of boron isotope fractionation in seawater. *Earth and Planetary Science Letters*, *248*(1-2), pp.276-285.

Larson, T.E., Sollo Jr, F.W. and McGurk, F.F., 1973. Complexes affecting the solubility of calcium carbonate in water. ISWS Contract Report CR 145.

Lewis, E.R. and Wallace, D.W.R., 1998. *Program developed for CO2 system calculations* (No. cdiac: CDIAC-105). Environmental System Science Data Infrastructure for a Virtual Ecosystem (ESS-DIVE)(United States).

Li, M., Kump, L.R., Ridgwell, A., Tierney, J.E., Hakim, G.J., Malevich, S.B., Poulsen, C.J., Tardif, R., Zhang, H. and Zhu, J., 2024. Coupled decline in ocean pH and carbonate saturation during the Palaeocene–Eocene Thermal Maximum. *Nature Geoscience*, *17*(12), pp.1299-1305.

Mehrbach, C., Culberson, C.H., Hawley, J.E. and Pytkowicx, R.M., 1973. Measurement of the apparent dissociation constants of carbonic acid in seawater at atmospheric pressure 1. *Limnology and Oceanography*, *18*(6), pp.897-907.
Millero, F.J., 1979. The thermodynamics of the carbonate system in seawater. *Geochimica et Cosmochimica Acta*, *43*(10), pp.1651-1661.

Millero, F.J., 1983. The estimation of the pK∗ HA of acids in seawater using the Pitzer equations. *Geochimica et Cosmochimica Acta*, *47*(12), pp.2121-2129.

https://doi.org/10.5194/egusphere-2025-5564
Preprint. Discussion started: 10 February 2026

Millero, F.J. and Schreiber, D.R., 1982. Use of the ion pairing model to estimate activity coefficients of the ionic components of natural waters. *American Journal of Science*, *282*(9), pp.1508-1540.

Millero, F.J., 1982. The effect of pressure on the solubility of minerals in water and seawater. *Geochimica et Cosmochimica Acta*, *46*(1), pp.11-22.

Millero, F.J. and Thurmond, V., 1983. The ionization of carbonic acid in Na-Mg-Cl solutions at 25° C. *Journal of Solution Chemistry*, 12, pp.401-412.

Millero, F.J. and Pierrot, D., 1998. A chemical equilibrium model for natural waters. *Aquatic Geochemistry*, *4*(1), pp.153-199.

Millero, F.J., Pierrot, D., Lee, K., Wanninkhof, R., Feely, R., Sabine, C.L., Key, R.M. and Takahashi, T., 2002. Dissociation constants for carbonic acid determined from field measurements. *Deep Sea Research Part I: Oceanographic Research Papers*, *49*(10), pp.1705-1723.

Morel, F. and Morgan, J., 1972. Numerical method for computing equilibriums in aqueous chemical systems. *Environmental Science & Technology*, *6*(1), pp.58-67.

Morse, J.W., Arvidson, R.S. and Lüttge, A., 2007. Calcium carbonate formation and dissolution. *Chemical Reviews*, *107*(2), pp.342-381.

Mucci, A., 1983. The solubility of calcite and aragonite in seawater at various salinities, temperatures, and one atmosphere total pressure. *American Journal of Science*, *283*(7), pp.780-799.

Ödalen, M., Nycander, J., Ridgwell, A., Oliver, K.I., Peterson, C.D. and Nilsson, J., 2020. Variable C/P composition of organic production and its effect on ocean carbon storage in glacial-like model simulations. *Biogeosciences*, *17*(8), pp.2219-2244.

Orr, J.C., Epitalon, J.M. and Gattuso, J.P., 2015. Comparison of ten packages that compute ocean carbonate chemistry. *Biogeosciences*, *12*(5), pp.1483-1510.

Orr, J.C., Epitalon, J.M., Dickson, A.G. and Gattuso, J.P., 2018. Routine uncertainty propagation for the marine carbon dioxide system. *Marine Chemistry*, *207*, pp.84-107.

Rae, J.W., Zhang, Y.G., Liu, X., Foster, G.L., Stoll, H.M. and Whiteford, R.D., 2021. Atmospheric CO2 over the past 66 million years from marine archives. *Annual Review of Earth and Planetary Sciences*, *49*.

Raitzsch, M., Hain, M., Henehan, M., and Gattuso, J.-P., 2022. Seacarbx -529 seacarb extension for deep-time carbonate system calculations. Zenodo. doi: 10530 .5281/zenodo.5909811

https://doi.org/10.5194/egusphere-2025-5564
Preprint. Discussion started: 10 February 2026

Reinhard, C.T., Olson, S.L., Kirtland Turner, S., Pälike, C., Kanzaki, Y. and Ridgwell, A., 2020. Oceanic and atmospheric methane cycling in the cGENIE Earth system model–release v0. 9.14. *Geoscientific Model Development*, *13*(11), pp.5687-5706.

Ridgwell, A. J. (2001), Glacial-interglacial perturbations in the global carbon cycle, Ph.D. thesis, Univ. of East Anglia at Norwich, Norwich, UK.

Ridgwell, A., Hargreaves, J.C., Edwards, N.R., Annan, J.D., Lenton, T.M., Marsh, R., Yool, A. and Watson, A., 2007. Marine geochemical data assimilation in an efficient Earth System Model of global biogeochemical cycling. *Biogeosciences*, *4*(1), pp.87-104.

Ridgwell, A., Reinhard, C., van de Velde, S., Adloff, M., Monteiro, F., Camillalxy98, Vervoort, P., Kanzaki, Y., Ward, B., Hülse, D., Wilson, J., Li, M., InkyANB, Tangirala, R. T., & Kirtland Turner, S., 2025. genie-model/cgenie.cookie: Adloff_et_al.GMDD.2025 (v0.9.90). Zenodo [code]. https://doi.org/10.5281/zenodo.17537316

Ridgwell, A., 2025. genie-model/cookiedoc: v0.9.90 (v0.9.90). Zenodo [code]. https://doi.org/10.5281/zenodo.17537474

Si, W., Herbert, T., Wu, M. and Rosenthal, Y., 2023. Increased Biogenic Calcification and Burial Under Elevated pCO2 During the Miocene: A Model-Data Comparison. *Global Biogeochemical Cycles*, *37*(6), p.e2022GB007541.

Sillen, L.G., 1961. The physical chemistry of seawater. In Oceanography—Invited Lectures Presented at the International Oceanography Congress, ed. M Sears, pp. 549–81. Washington, DC: Am. Assoc. Adv. Sci. Publ. 67.

Stanley, S.M. and Hardie, L.A., 1998. Secular oscillations in the carbonate mineralogy of reef-building and sediment-producing organisms driven by tectonically forced shifts in seawater chemistry. *Palaeogeography, Palaeoclimatology, Palaeoecology*, *144*(1-2), pp.3-19.

Stanley, S.M., Ries, J.B. and Hardie, L.A., 2005. Seawater chemistry, coccolithophore population growth, and the origin of Cretaceous chalk. *Geology*, *33*(7), pp.593-596.

Stanley, S.M., 2006. Influence of seawater chemistry on biomineralization throughout Phanerozoic time: Paleontological and experimental evidence. *Palaeogeography, Palaeoclimatology, Palaeoecology*, *232*(2-4), pp.214-236.

Stefánsson, A., Lemke, K.H., Bénézeth, P. and Schott, J., 2017. Magnesium bicarbonate and carbonate interactions in aqueous solutions: An infrared spectroscopic and quantum chemical study. Geochimica et Cosmochimica Acta, 198, pp.271-284.

Timofeeff, M.N., Lowenstein, T.K., Da Silva, M.A.M. and Harris, N.B., 2006. Secular variation in the major-ion chemistry of seawater: Evidence from fluid inclusions in Cretaceous halites. *Geochimica et Cosmochimica Acta*, *70*(8), pp.1977-1994.

https://doi.org/10.5194/egusphere-2025-5564
Preprint. Discussion started: 10 February 2026

Turner, D.R., Achterberg, E.P., Chen, C.T.A., Clegg, S.L., Hatje, V., Maldonado, M.T., Sander, S.G., Van den Berg, C.M. and Wells, M., 2016. Toward a quality-controlled and accessible Pitzer model for seawater and related systems. *Frontiers in Marine Science*, *3*, p.139.

Tyrrell, T. and Zeebe, R.E., 2004. History of carbonate ion concentration over the last 100 million years. *Geochimica et Cosmochimica Acta*, *68*(17), pp.3521-3530.

Zeebe, R.E. and Tyrrell, T., 2018. Comment on "The effects of secular calcium and magnesium concentration changes on the thermodynamics of seawater acid/base chemistry: Implications for Eocene and Cretaceous ocean carbon chemistry and buffering" by Hain et al.(2015). *Global Biogeochemical Cycles*, *32*(5), pp.895-897.

Zeebe, R.E. and Tyrrell, T., 2019. History of carbonate ion concentration over the last 100 million years II: Revised calculations and new data. *Geochimica et Cosmochimica Acta*, *257*, pp.373-392.

Wanninkhof, R., 1992. Relationship between wind speed and gas exchange over the ocean. *Journal of Geophysical Research: Oceans*, *97*(C5), pp.7373-7382.

Whiteford, R., Branson, O. and Mayk, D., 2025. Using Kgen to generate cross-verified apparent equilibrium constants (K∗'s) for Palaeoseawater carbonate chemistry. *Geochemistry, Geophysics, Geosystems*, *26*(6), p.e2023GC011417.